n-octane reforming over alumina-supported Pt, Pt–Sn and Pt–W catalysts

M.C. Rangel [a], L.S. Carvalho [a], P. Reyes [b], J.M. Parera [c] and N.S. Fígoli [c]

[a] *Departamento de Físico-Química, Instituto de Química, Universidade Federal da Bahia, Campus Universitário de Ondina, Federacao, CEP 41170280, Salvador, BA, Brazil*

[b] *Departamento de Físico-Química, Facultad de Ciencias Químicas, Universidad de Concepción, Casilla 160-C, Concepción, Chile*

[c] *Instituto de Investigaciones en Catálisis y Petroquímica (INCAPE), FIQ, UNL-CONICET, Santiago del Estero 2654, 3000 Santa Fe, Argentina*

E-mail: nfigoli@fiqus.unl.edu.ar

Received 20 June 1999; accepted 22 November 1999

Pt, Pt–Sn and Pt–W supported on γ-Al_2O_3 were prepared and characterized by H_2 chemisorption, TEM, TPR, test reactions of n-C_8 reforming (500 °C), cyclohexane dehydrogenation (315 °C) and n-C_5 isomerization (500 °C), and TPO of the used catalysts. Pt is completely reduced to Pt^0, but only a small fraction of Sn and of W oxides are reduced to metal. The second element decreases the metallic properties of Pt (H_2 chemisorption and dehydrogenation activity) but increases dehydrocyclization and stability. In spite of the large decrease in dehydrogenation activity of Pt in the bimetallics, the metallic function is not the controlling function of the bifunctional mechanisms of dehydrocyclization. Pt–Sn/Al_2O_3 is the best catalyst with the highest acid to metallic functions ratio (due to its lower metallic activity) presenting a xylenes distribution different from the other catalysts. The acid function of Pt–Sn/Al_2O_3 is tuned in order to increase isomerization and cyclization and to decrease cracking, as compared to Pt and Pt–W.

Keywords: bimetallic catalysts, metal and acid functions, n-C_8 reforming

1. Introduction

Dehydrocyclization of paraffins is one of the main reactions during naphtha reforming, because it increases the octane number and produces valuable aromatic hydrocarbons (benzene, toluene and xylenes). The reaction rate is favored at high temperature and at low pressure, conditions under which catalyst deactivation is important, therefore being necessary the use of stable catalysts. Different formulations were proposed in order to achieve a better stability and to increase the selectivity to aromatics of the traditional Pt/Al_2O_3 catalyst. One of them is the bimetallic Pt–Sn/Al_2O_3 catalyst, which is particularly attractive because it can be used under a low hydrogen pressure and continuous regeneration, being reintroduced in the reactor with simple pretreatments after regeneration [1,2]. According to literature [3], when reducing the Pt and Sn precursors supported on Al_2O_3, a small part of Sn is reduced to the metallic state, and it can be alloyed to Pt. Another interesting system is Pt–W/Al_2O_3 due to its high selectivity to aromatics [4] and the stabilization effect of tungsten over platinum particles [5,6]. During its preparation, Al_2O_3 is impregnated with solutions of the Pt and W precursors; the material is then dried at 120 °C and calcined and reduced at 500 °C. According to Kadkhodayan and Brenner [7], the reduction of WO_3 supported on Al_2O_3 is very difficult, meanwhile masic WO_3 is completely reduced. This means that there is a strong interaction of WO_3 with Al_2O_3. Tungsten bronzes, for instance $H_{0.5}WO_3$, can also be produced during reduction [8].

The objective of this paper is to prepare, characterize and compare the catalytic activity, selectivity and stability of Pt, Pt–Sn and Pt–W/Al_2O_3 catalysts during the n-octane reforming and to deduce the modifications produced in the catalytic functions of Pt/Al_2O_3 by the introduction of tin or tungsten.

2. Experimental

2.1. Catalyst preparation

The 0.3% M/Al_2O_3 (M = Pt, Sn or W) and 0.3% Pt–0.3% N/Al_2O_3 (N = Sn or W) catalysts were prepared by wet impregnation or coimpregnation, respectively, from H_2PtCl_6, $SnCl_2$ and $(NH_4)_2WO_4$ aqueous solutions, followed by drying at 120 °C and calcination at 500 °C. γ-Al_2O_3 Ketjen CK300 (S_g = 180 $m^2\,g^{-1}$) 35–80 mesh, previously calcined at 500 °C, was used as support. A 20% H_2O_2 solution was added to the tungsten-containing catalysts to avoid paratungstic acid precipitation and to improve platinum dispersion [9].

2.2. Catalyst characterization

Platinum, tungsten and tin content of the different catalysts were determined by inductively coupled plasma atomic emission spectroscopy (ICP-AES). Temperature-programmed reduction (TPR) and H_2 chemisorption of the samples were carried out in a Micromeritics TPD/TPR 2900 equipment. The TPR experiments were performed heating

at 10 °C min^{-1} and using a 5% hydrogen in nitrogen mixture. TEM was used to observe the supported metal particles. These experiments were performed in a Jeol model JEM-1200 EX II system. The samples were prepared by extractive replica. Previous to the catalytic test, 0.3 g of catalyst were heated in N_2 (40 ml min^{-1}) up to 500 °C and reduced at this temperature in a stream of H_2 (50 ml min^{-1}) for 2 h in a flow reactor. Then, the catalytic activity and selectivity in n-octane reforming were measured at 500 °C, H_2 : n-octane (molar) = 19 and atmospheric pressure during 6 h in the same reactor. n-octane was introduced passing a 12 ml min^{-1} hydrogen flow over a saturator containing the hydrocarbon kept at 45 °C. Reactants and products were analyzed on-line using a Varian 3600 CX gas chromatograph. Thermal-programmed oxidation of the used catalysts was carried out in order to characterize the coke deposited during reaction.

The activity of the metallic function was followed by the cyclohexane dehydrogenation reaction carried out at 315 °C and H_2 : cyclohexane (molar) = 10 for 3 h using a continuous-flow reactor, and 0.1 g of 35–80 mesh catalyst. The reactor feed was a 100 ml min^{-1} hydrogen flow saturated in cyclohexane kept at 20 °C. Reaction products were analyzed by on-line gas chromatography.

n-pentane isomerization was used to follow the activity of the acid function. The reaction was carried out at 500 °C, WHSV = 4.5 h^{-1}, H_2 : n-pentane (molar) = 6 and 10 atm during 2 h, using 0.15 g of 35–80 mesh catalyst. Product analysis was carried out by on-line gas chromatography.

3. Results and discussion

Table 1 shows the composition as well as the H_2 chemisorption capacity, metallic dispersion and mean platinum particle size of the different catalysts. All the catalysts have the same chloride content, around 0.7%. The Pt dispersion (H/Pt) and mean particle size calculated from H_2 chemisorption data show that the addition of the second element produces a large decrease in dispersion and an increase in particle size. But this is not shown by the TEM measurements; the addition of tin does not produce any modification in the particle size and the addition of W produces an increase of only 10%. Then, hydrogen chemisorption is not useful for the calculation of metallic dispersion or particle size in bimetallic catalysts because, due to electronic and/or geometrical effects of the second element on Pt, its chemisorption capacity is greatly decreased. The H_2 chemisorption is useful only to calculate metallic dispersion and crystal size of monometallic Pt crystals.

Figure 1 shows the TPR profiles of the catalysts. Al_2O_3 (not shown) does not show reduction peaks up to 700 °C. Pt/Al_2O_3 shows a peak centered at about 230 °C attributed to the reduction of surface oxychlorated platinum species [10,11], and another peak centered at about 370 °C ascribed to platinum species in strong interaction with the support [12], to Pt_xAlO_x species or to the formation of the alloy Pt_3Al [13]. Sn/Al_2O_3 and W/Al_2O_3 (not shown) are reduced above 500 °C. Pt–Sn/Al_2O_3 presents two peaks, the first at 260 °C can be attributed to the reduction of platinum oxide and of some Sn oxide in its vicinity or previously alloyed, and another peak around 500 °C corresponding to Sn oxide reduction [14]. It can be observed a shift in the platinum reduction peak from 230 to 260 °C that can be

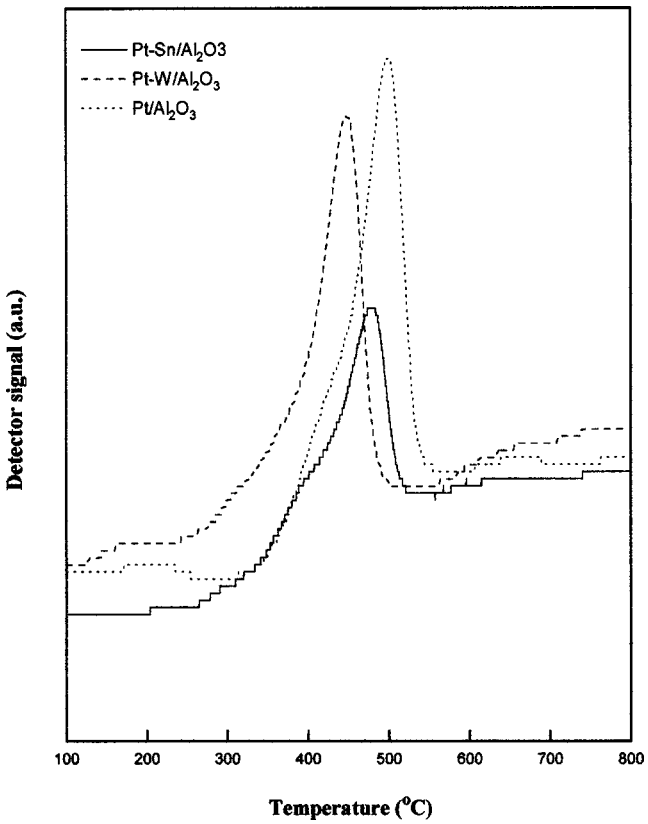

Figure 1. Temperature-programmed reduction (TPR) profiles of the catalysts.

Table 1
Composition, hydrogen chemisorption capacity, metallic dispersion and mean platinum particle size of the different catalyst samples.

Catalyst	Composition (%)			H_2 chem.	H/Pt	Mean Pt particle size (nm)	
	Pt	Sn	W	(μmol g^{-1})		H_2 chem.	TEM
Pt/Al_2O_3	0.28	0	0	12.7	0.50	1.7	1.6
Pt–Sn/Al_2O_3	0.20	0.29	0	1.77	0.10	8.5	1.6
Pt–W/Al_2O_3	0.23	0	0.26	1.85	0.26	3.3	1.8
Sn/Al_2O_3	0	0.30	0	0	–	–	–
W/Al_2O_3	0	0	0.30	0	–	–	–

assigned to a Pt–Sn interaction, and the disappearance of the Pt reduction peak at 370 °C. This can be due to the weakening of the interaction of Pt species with the support produced by the presence of tin oxides, which allows the total reduction of Pt in the first peak. The TPR profile of Pt–W/Al_2O_3 presents the same peaks as Pt/Al_2O_3 and a shoulder at 460 °C, possibly due to the reduction of WO_3 species catalyzed by the presence of platinum [15]. It can be considered that most of tungsten oxide species remain as WO_x in strong interaction with the support. In all cases platinum was completely reduced during the TPR, and the hydrogen consumption indicated that platinum was in the 4+ oxidation state.

Table 2 shows the theoretical and experimental consumptions of hydrogen during the TPR. Theoretical values correspond to the hypothetical case that the three elements are reduced to the metallic, zero valence, state. Experimental values indicate that a small fraction of Sn and W oxides are reduced. According to what was quoted in section 1, a small part of the H_2 consumption corresponds to the reduction of Sn or W to the metallic state. The other part corresponds to the reduction to lower valence oxides or, in the case of W, to the formation of hydrogen tungsten bronzes.

Table 2
Hydrogen consumption during the TPR experiments.

Catalyst	H_2 consumption (μmol g^{-1})	
	Theoretic	Experimental
Pt/Al_2O_3	29.0	29.0
Sn/Al_2O_3	50.0	13.5
W/Al_2O_3	48.0	10.0
Pt–Sn/Al_2O_3	69.5 (Pt = 20.5; Sn = 49)	35.0 (Pt = 20.5; Sn = 14.5)
Pt–W/Al_2O_3	65.6 (Pt = 23.6; W = 42)	34.2 (Pt = 23.6; W = 10.6)

During the commercial operation of reforming, the temperature is lower than at the end of the TPR experiment and the percentage of reduction of the second element should be smaller. Then, according to these results, the conventional designation as "bimetallic catalyst" for Pt–Sn/Al_2O_3 and Pt–W/Al_2O_3 does not mean that Pt and the second element are in the metallic, zero valence, state. Only Pt is reduced to Pt^0, the second element is only partially in the metallic state influencing the properties of Pt. Most part of the second element remains as oxides interacting with Pt and with Al_2O_3. Mixed compounds could be produced on the support that can influence its acid properties and the Pt–support interaction.

Figure 2 and table 3 show the total n-octane conversion as a function of time for the three catalysts. At the beginning of the run, the n-C_8 conversion on the three catalysts is 100%, but the operation is unstable, mainly in Pt/Al_2O_3 due to its rapid deactivation. The activity in hydrogenolysis of Pt/Al_2O_3 is high, producing large amounts of C_1 and C_2, and also of benzene and toluene which are products of the hydrogenolysis of C_8 aromatics. For this reason, first data shown in table 3 are at 1 h time on stream (TOS), when the catalyst is more stabilized and Pt/Al_2O_3 is partially deactivated. It can be observed that Pt/Al_2O_3 is the catalyst most

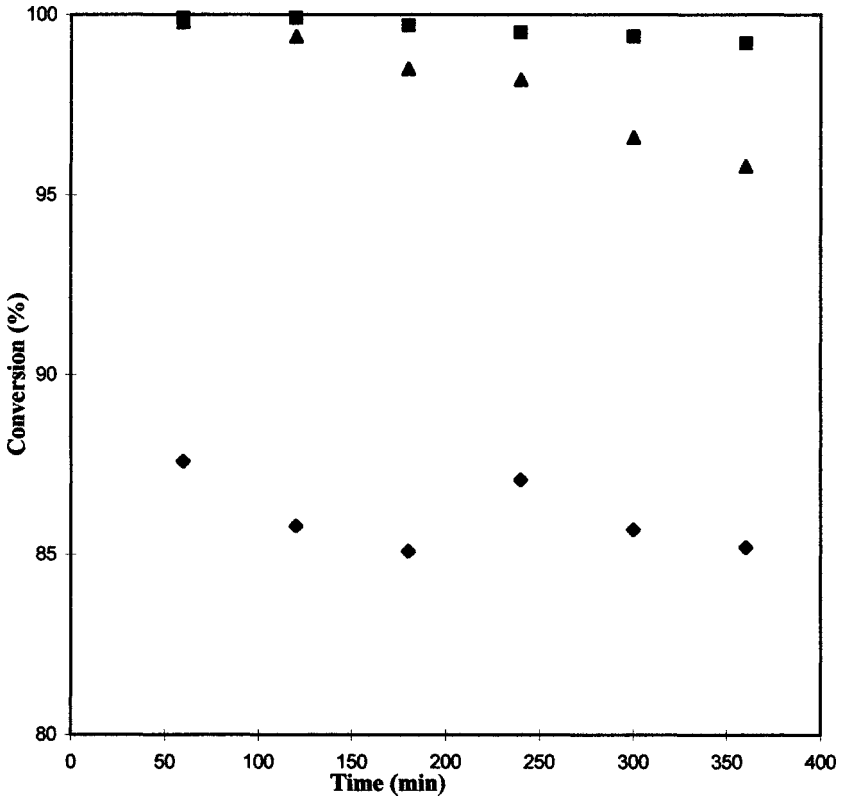

Figure 2. Conversion of n-C_8 as a function of time: (■) Pt–Sn/Al_2O_3, (▲) Pt–W/Al_2O_3 and (♦) Pt/Al_2O_3.

Table 3
Conversion of n-C_8 (mol n-C_8 converted to the product per 100 mol n-C_8 fed) to some products at two TOS.

Product	Pt/Al_2O_3		$Pt–Sn/Al_2O_3$		$Pt–W/Al_2O_3$	
(%)	1 h	6 h	1 h	6 h	1 h	6 h
Methane	0.2	0.2	0.1	0.1	0.4	0.3
Ethane	0.6	0.7	0.2	0.3	0.8	0.9
Propane	1.1	1.2	0.3	0.3	2.9	1.2
n-butane + i-butane	1.4	1.5	0.3	0.5	0.8	0.8
C_4 olefins	0.2	0.3	0.1	0.1	0.4	0.5
n-pentane + i-pentane	1.0	1.0	0.2	0.4	1.8	1.9
n-hexane + i-hexane	0.2	0.2	0.1	0.1	0.1	0.3
Cyclopentane	0.1	0.1	–	0.1	0.2	0.2
Methylcyclopentane	0.1	0.2	–	–	0.1	0.2
Benzene	1.3	1.1	0.9	1.0	2.4	1.6
Toluene	3.0	3.0	1.2	1.5	3.8	3.1
m-xylene	26.0	23.3	28.4	30.4	25.4	25.9
o-xylene	19.9	12.4	31.4	29.9	23.4	20.4
p-xylene	8.6	6.2	9.2	10.2	12.1	10.9
Ethylbenzene	10.3	5.8	14.4	14.2	15.6	11.7
Total C_8 arom.	64.8	47.7	83.4	84.7	76.5	68.9
Total n-C_8 conv.	87.6	85.2	99.9	99.2	99.8	95.8

rapidly deactivated and that $Pt–Sn/Al_2O_3$ is the most active and stable one. These results were confirmed repeating the runs with half the amount of catalyst (0.15 g). Total conversions of n-C_8 at 1 and 6 h TOS were 36 and 33.0% for Pt/Al_2O_3, 53 and 50% for $Pt–Sn/Al_2O_3$ and 46 and 45% for $Pt–W/Al_2O_3$.

Figure 3 shows the TPO profiles of the catalysts after the n-octane reaction. The amount of coke deposited over the bimetallic catalysts was lower than on Pt/Al_2O_3. Burch and Garla [16] have proposed that an electronic transfer from Sn to Pt occurs, decreasing the Pt–C interaction and increasing the resistance to coke deposition. For $Pt–W/Al_2O_3$, M'Boungou et al. [15] considered that the irreversible carbon adsorption could be suppressed by the formation of surface carbide species as well as by the improvement in the hydrogenation of carbon residues associated with a modification in the chemisorption of hydrogen. The shift to lower temperatures in the TPO peak of $Pt–W/Al_2O_3$ suggests a less polymerized coke when compared to the other catalysts. This can be ascribed, as it will be shown later, to the higher activity in hydrogenolysis of $Pt–W/Al_2O_3$.

Table 3 shows the conversion of n-C_8 to the most interesting (from a mechanistic point of view) products at 1 h TOS and at the end of the run, 6 h TOS. The formation of C_1 and C_2 can be taken as a measure of the activity in hydrogenolysis of the metallic function of the catalysts; their values are the lowest for $Pt–Sn/Al_2O_3$ and the highest for $Pt–W/Al_2O_3$ and, consequently, the formation of benzene and toluene by hydrogenolysis of produced xylenes shows the same behavior. Several authors [17] found that the addition of tungsten to Pt/Al_2O_3 increases the activity in hydrogenolysis of the catalyst. This can occur through the formation of hydrogen–tungsten compounds [15], being favored hydrogenolysis, hydrocracking and other hydrogenation reactions. Although the formation of metallic W should be very small, W produces carbides under the reaction conditions, with hydrogenolytic properties similar to those of Pt [18]. Cracking of n-C_8 on the acid sites of the catalysts produces the C_3, C_4 and C_5 hydrocarbons. Lowest values of these products correspond to $Pt–Sn/Al_2O_3$. This means that the part of the acid function which is able to crack n-C_8 is partially neutralized by Sn oxides, whereas the part that controls the bifunctional mechanism of n-C_8

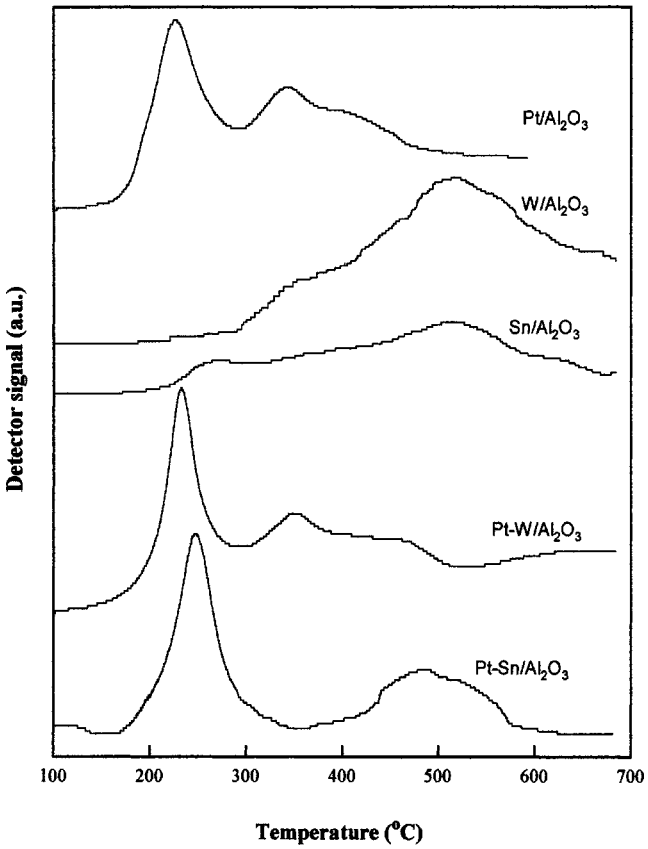

Figure 3. Temperature-programmed oxidation (TPO) of the catalysts used in n-C_8 reforming.

dehydrocyclization is increased because, as seen below, the production of xylenes is quite higher on Pt–Sn/Al_2O_3. The acidity of this catalyst is tuned or balanced in order to produce more cyclization than cracking. The basicity of Sn oxides decreases the strong acidity (able to crack hydrocarbons) to a weaker acidity more able to catalyze cyclization.

It is interesting to analyze the C_8 aromatics distributions shown in table 3. According to Davis and Venuto [19], when the catalyst has only the metallic function, the cyclization of n-C_8 is produced by the direct C_6 ring closure, giving a mixture of ethylbenzene (EB) and o-xylene (oX). Our catalysts are bifunctional and the presence of the acid function adds isomerization and cracking capacity to them. The dehydrocyclization activity of the bifunctional catalysts is quite higher than that of the non-acid (only metallic) catalysts [20]. Paraffin isomerization is a very rapid reaction when compared to dehydrocyclization and hydrocracking over bifunctional catalysts [21]. n-C_8 is firstly isomerized, being then the C_8 isomers dehydrocyclized. Over bifunctional catalysts, the cyclization of the carbon chain occurs mainly on the acid function through the formation of a five-carbon or a six-carbon ring intermediate [20]. It seems the acidity of the Al_2O_3 support does not allow the isomerization of the C_8 aromatics produced as to reach equilibrium [20]. The thermodynamic equilibrium composition of the C_8 aromatics indicates m-xylene (mX) (near 50% of the equilibrium mixture of C_8 aromatics) as its main component, similar amounts of oX and p-xylene (pX) (about 20% each) and EB as the smallest fraction (near 10%). Experimental fractions of mX and pX (shown in table 3) are lower than the ones at equilibrium, and those of oX and EB are higher for all our catalysts and TOS. The same occurs with the runs with half the amount of the catalyst quoted above.

The C_8 aromatics composition depends on the n-C_8 isomerization produced before the dehydrocyclization step. The isomerization of n-C_8 produces mainly 2-methylheptane (2-MHp) and 3-methylheptane (3-MHp), because 4-methylheptane (4-MHp) has a low stability [20]. If the cyclization occurs by the direct C_6 ring closure, n-C_8 would produce a mixture of oX and EB, as shown in figure 4. Figure 4 shows that if the dehydrocyclization pathway is through a C_5 ring closure, n-C_8 will produce a mixture of propylcyclopentane and 1-methyl, 2-ethyl cyclopentane.

The C_5 ring closure is not drawn in figure 4 to avoid blurring, but the products are indicated in the text. Considering only the C_6 ring closure, figure 4 shows that 2-MHp would produce only mX, 3-MHp would produce a mixture of pX, oX and EB and 4-MHp would produce only mX. Table 3 shows for Pt/Al_2O_3 and Pt–W/Al_2O_3 that the main C_8 aromatic is mX, followed by oX, lower values of EB and the lowest value corresponds to pX. This suggests 2-MHp as the main isomer dehydrocyclized, followed by n-C_8 and 3-MHp. In the case of Pt–Sn/Al_2O_3, the selectivity is different, the ratios oX/mX and EB/pX are higher than in the other catalysts, indicating a larger dehydrocyclization of n-C_8. Pt–Sn/Al_2O_3 has the same behavior during the

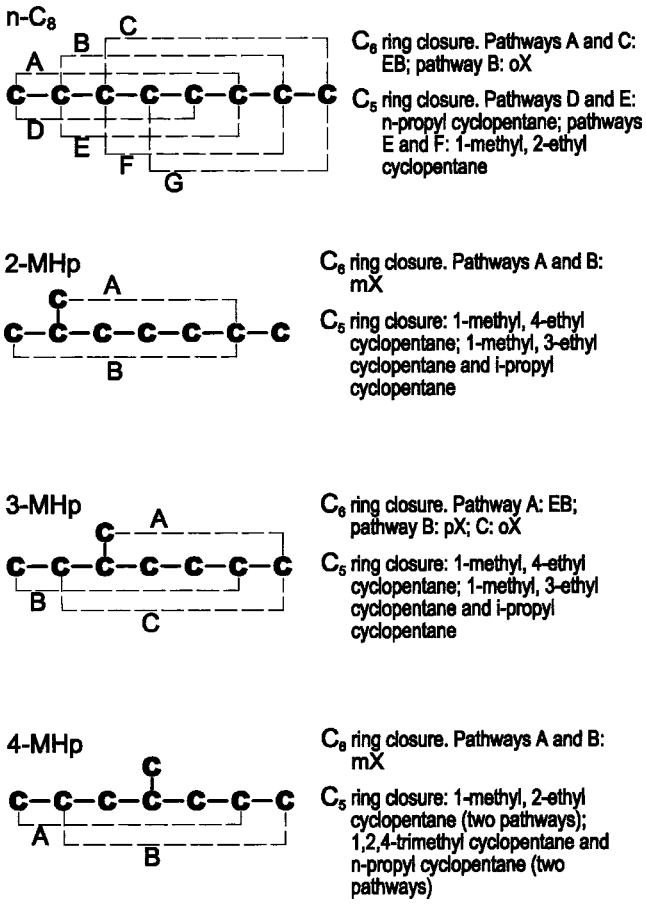

Figure 4. Scheme of octane dehydrocyclization.

runs at low conversion. The smaller formation of EB, as compared to oX, can be due to different energetic requirements for C–H bond rupture [22]. The C–H bond strength of primary hydrogen (–CH_3) is higher than the one of secondary hydrogen (–CH_2–) and it can be expected that its rupture to form a C–C bond will be more difficult. The formation of EB from n-C_8 requires the rupture of one primary C–H bond while the formation of oX requires only the rupture of secondary bonds. From 3-MHp, the formation of EB requires the rupture of two primary bonds while the formation of oX or pX only requires the rupture of one primary bond. According to the results, if the formation of C_8 aromatics occurs by direct C_6 ring closure of the C_8 alkanes, the most abundant C_8 isoalkane intermediate will be 2-MHp (main product mX), followed by n-C_8 (second product oX) and the less abundant 3-MHp (small amount of pX). But, as quoted above, the C_5 ring closure of paraffins over bifunctional catalysts can occur together with the C_6 ring closure. The alkylcyclopentanes resulting from the C_5 ring closure on the acid sites require an additional C_5 to C_6 ring enlargement step, also on the acid sites, in order to form the six-membered ring. By dehydrogenation of that ring on the metal sites, the C_8 aromatics are produced. The C_5 ring closure has more steps than the C_6 ring closure and can produce a different distribution of C_8 aromatics. According to the hydrocarbons chain length, the cyclization

through a C_6 ring closure is the most feasible under our operational conditions.

It is also interesting to analyze the production of cyclopentane and methylcyclopentane. The lowest values of these C_5 naphthenes are produced by Pt–Sn/Al_2O_3. These naphthenes are great coke precursors, but in our case they are not the main cause of coke deposition because Pt–W/Al_2O_3 produces more C_5 naphthenes but less coke than Pt/Al_2O_3. Perhaps, the small amount of C_5 ring compounds on Pt–Sn/Al_2O_3 is an indication that the cyclization by means of a C_5 ring closure is very small over this catalyst.

Test reactions were performed in order to compare the metallic and acid functions of the catalysts. Table 4 presents the metallic function activity of the three catalysts measured as the activity in cyclohexane dehydrogenation. This reaction is very selective and stable in the 3 h run. The dehydrogenation reaction does not demand a special metallic structure or particle size, being a non-demanding reaction in the sense of Boudart et al. [23]. Then, the activity values are only a function of the number of exposed platinum atoms. Sn/Al_2O_3 and W/Al_2O_3 do not show activity in dehydrogenation. Metallic Sn has no hydrocarbons hydrogenating or dehydrogenating activity, neither hydrogen chemisorption ability. Metallic tungsten has activity in hydrogenation, but under the reduction conditions used here, tungsten remains mainly as WO_x species, without hydrogen chemisorption or activity in dehydrogenation. Table 4 shows that Pt/Al_2O_3 has a high activity in dehydrogenation and that the bimetallic catalysts have a low activity due to electronic and/or geometric interaction of the second element over Pt. It can be considered that the most important is the electronic effect because the small amount of the second element reduced and possibly alloyed to Pt could not be able to produce the large decrease in the metallic properties of Pt (H_2 chemisorption, dehydrogenation reaction, hydrogenolysis and coke precursors formation). Although the bimetallic catalysts have a metallic activity quite lower than Pt/Al_2O_3, it is seen in table 3 that their dehydrocyclization activities are not lower, but higher. This indicates that the metallic function is not the controlling one in alkane dehydrocyclization on bifunctional catalysts.

Table 4
Benzene production from cyclohexane dehydrogenation.

Catalyst	Benzene (%)
Pt/Al_2O_3	27.2
Pt–Sn /Al_2O_3	0.7
Pt–W/Al_2O_3	3.8

Table 5 shows the products distribution during the n-pentane reaction for the different catalysts. There is no aromatics formation using n-C_5 as feed, the main products being isomeric paraffins. It is accepted that the isomerization mechanism for these catalysts is bifunctional metal–acid [24]. The reaction begins with the paraffin dehydrogenation on the metallic sites, the olefin so produced is isomerized on the acid sites and the isoolefin is hydrogenated on the metal sites. The reaction mechanism is controlled by the acid function [25] and the formation of isopentane can be taken as a measure of that function. The formation of C_3 can also be taken as a measure of the acid function. Another product of the n-pentane reaction is methane (C_1), a typical product of the hydrogenolysis on the metallic function [26]. The C_3/C_1 molar ratio is usually taken as a measure of the balance between the acid and metal functions of the catalyst. The cyclization of n-C_5 to cyclopentane is the smallest on Pt–Sn/Al_2O_3, in agreement with the lower production of cyclopentane and methylcyclopentane from n-C_8 commented above, showing the low capacity of Pt–Sn/Al_2O_3 to produce the C_5 ring closure. Table 6 presents n-C_5 conversion, selectivity to C_1 and i-C_5, and the C_3/C_1 molar ratio, calculated from data in table 5, for Pt/Al_2O_3 and the bimetallic catalysts. Tables 5 and 6 show that, from the first to the last chromatographic analysis, there exists a rapid catalyst deactivation. The conversion as well as the stability of Pt–Sn/Al_2O_3 are higher than those of the other catalysts. C_1 and C_3 decrease during the run, but the former decreases more rapidly due to the fact that, at the beginning of the run, the metallic function is more rapidly deactivated than the acid function; consequently the C_3/C_1 ratio increases [21]. The behavior of the catalysts during n-C_5 isomerization is similar to the one for n-C_8 dehydrocyclization: Pt–Sn/Al_2O_3 is the most active and selective catalyst, presents the lowest metallic function and the highest acid to metal function ratio.

The comparison of the catalytic functions of Pt–Sn/Al_2O_3 to those of Pt/Al_2O_3 is useful. The presence of Sn greatly affects the metallic activity of Pt, the dehydrogenation capacity of Pt–Sn/Al_2O_3 is 39 times lower than

Table 5
Composition (weight %) at the reactor outlet during the isomerization of n-pentane at two TOS.

Catalyst	Time (min)	C_1	C_2	C_3	$C_4^=$	i-C_4	n-C_4	i-C_5	n-C_5	i-C_6	Cyclopentane
Pt/Al_2O_3	5	0.9	1.5	2.9	0.4	0.9	1.7	14.9	61.8	13.3	1.7
	120	0.4	0.9	2.2	0.8	0.9	0.3	6.9	74.6	11.2	1.7
Pt–Sn/Al_2O_3	5	0.2	1.1	3.0	0.2	0.8	1.0	30.3	43.3	19.3	0.7
	120	0.1	1.6	1.3	0.2	0.2	0.5	17.6	59.6	18.6	0.3
Pt–W/Al_2O_3	5	0.7	1.4	2.7	0.3	0.8	1.5	17.8	54.9	16.8	2.9
	120	0.1	0.3	1.0	0.6	1.4	0.4	8.4	71.7	14.0	2.0
W/Al_2O_3	5	0.1	0.4	0.5	0.3	1.6	0.0	0.3	95.4	1.2	0.1
Sn/Al_2O_3	5	0.0	0.2	0.1	0.0	0.2	0.0	0.2	98.9	0.3	0.1

Table 6
Conversion, selectivity to C_1, C_3/C_1 molar ratio and selectivity to n-pentane isomers during n-pentane isomerization at two TOS.[a]

Catalyst	Time (min)	Conversion (%)	Sel. C_1 (%)	C_3/C_1 (molar)	Sel. i-C_5 (%)
Pt/Al_2O_3	5	38.3	2.4	1.1	39.1
	120	25.4	1.6	2.0	27.4
$Pt–Sn/Al_2O_3$	5	56.6	0.4	5.4	53.4
	120	39.3	0.2	6.6	44.7
$Pt–W/Al_2O_3$	5	45.1	1.6	1.4	39.6
	120	28.3	0.4	3.0	29.7

[a] Sel. C_i = selectivity to C_i = n-C_5 conversion to $C_i \times 100/$total n-C_5 conversion.

that of Pt/Al_2O_3 (table 4), but the rate of the bifunctional mechanism of dehydrocyclization is not decreased. Due to the very high rate of alkane dehydrogenation under the operational conditions used, the alkenes produced on these catalysts are in thermodynamic equilibrium and dehydrogenation is not the controlling step of the dehydrocyclization bifunctional mechanism. The presence of Sn oxides affects the acidity of the support. The formation of C_3–C_5 alkanes from n-C_8 (by cracking at the middle of the chain) on $Pt–Sn/Al_2O_3$ is smaller here than on the other catalysts, because cracking reactions require strong acid sites. The formation of aromatic hydrocarbons is the largest on $Pt–Sn/Al_2O_3$. This reaction is produced by a bifunctional mechanism that includes isomerization or cyclization of unsaturated hydrocarbons on acid sites. The required acidity of these sites is not so strong as the one for cracking; then, it can be considered that the Sn oxides decrease the strong acidity of the support to a more convenient value for isomerization or cyclization than for cracking.

4. Conclusions

Hydrogen chemisorption and TPR profiles show Sn affects Pt more than W, and all Pt and only a small fraction of the second element are reduced to the metallic state. The second element remains mostly in an oxidized state influencing the support (acidity, metal–support interaction) and the metal (H_2 chemisorption, dehydrogenation activity).

The addition of Sn and W produces an increase in activity and stability to Pt/Al_2O_3, and also beneficial changes in selectivity during n-C_8 dehydrocyclization. The best catalyst is $Pt–Sn/Al_2O_3$, and the addition of tungsten produces minor modifications. The second element produces a large decrease in the metallic properties of Pt: the hydrogen adsorption capacity and the catalytic activity in cyclohexane dehydrogenation are greatly decreased. Nevertheless, the dehydrocyclization capacity remains very high.

The test reaction of the acid function, n-C_5 isomerization, follows the same pattern as the n-C_8 dehydrocyclization: $Pt–Sn/Al_2O_3$ is the best catalyst, and $Pt–W/Al_2O_3$ and Pt/Al_2O_3 are not very different. $Pt–Sn/Al_2O_3$ has the highest acid/metal ratio due to a larger decrease on the metal, producing less hydrogenolysis and more isomerization and cyclization.

Tin is the best modifier of the metallic function, because it decreases hydrogenolysis and the production of highly dehydrogenated coke precursors. The activity for dehydrogenation and hydrogenation is decreased; nevertheless, it is enough to produce sufficient alkenes in order to be a non-controlling function. Tin also modifies the acid function, tuning or balancing it in order to produce more cyclization by C_6 ring closure and to decrease cracking to C_3–C_5 and condensation to carbonaceous deposits.

Acknowledgement

LSC acknowledges CAPES. The financial assistance of FINEP, CNPq, CONICET, UNL and the trinational project from Vitae, Antorchas and Andes Foundations are also acknowledged.

References

[1] Y.-X. Li, K.L. Klabund and B.H. Davis, J. Catal. 128 (1991) 1.
[2] R. Srinivasan, L.A. Rice and B.H. Davis, J. Catal. 129 (1991) 257.
[3] B.H. Davis and G.J. Antos, in: *Catalytic Naphtha Reforming*, eds. G.J. Antos, A.M. Aitani and J.M. Parera (Dekker, New York, 1995) ch. 5, p. 153.
[4] V. Haensel, US Patent 2 957 819, UOP (1960).
[5] J.L. Contreras, Ph.D. thesis, Universidad Autónoma Metropolitana Iztapalapa, México (1960).
[6] J.L. Contreras, G.A. Fuentes and E.M.M. Domínguez, in: *Anal. XV Simp. Iberoam. Catal.*, Córdoba, Argentina, 1996, Vol. I, p. 1.
[7] A. Kadkhodayan and A. Brenner, J. Catal. 117 (1989) 311.
[8] C.L. Rollinson, *The Chemistry of Chromium, Molybdenum and Tungsten*, Pergamon Texts in Inorganic Chemistry, Vol. 21 (Pergamon, Oxford, 1973) p. 767.
[9] A.K. Aboul-Gheit and S.M. Abdel-Hamid, in: *Preparation of Catalysts VI. Scientific Bases for the Preparation of Heterogeneous Catalysts*, eds. G. Poncelet et al. (Elsevier, Amsterdam, 1995) p. 1131.
[10] T.F. Garetto, A. Borgna, E. Benvenuto and C.R. Apesteguía, in: *XII Symp. Iberoam. Catal.*, Rio de Janeiro, Brasil, 1990, Vol. I, p. 585.
[11] H. Lieske, G. Lietz, H. Spindler and J. Volter, J. Catal. 81 (1983) 8.
[12] K. Kunimore, Y. Ikeda, M. Soma and T. Uchijima, J. Catal. 79 (1983) 185.
[13] G. Den Otter and F.M. Dautzenberg, J. Catal. 53 (1978) 116.
[14] S. Stagg, W. Alvarez, D. Resasco, J.M. Parera and C.A. Querini, in: *Anal. XV Symp. Iberoam. Catal.*, Córdoba, Argentina, 1996, Vol. II, p. 1061.
[15] J.S. M'Boungou, J.L. Schmitt, G. Maire and F. Garin, Catal. Lett. 10 (1991) 391.

[16] R. Burch and L.C. Garla, J. Catal. 71 (1981) 360.
[17] E. Iglesia, J.E. Baumgartner, F.H. Ribeiro and M. Boudart, J. Catal. 131 (1991) 523.
[18] R.B. Levy and M. Boudart, Science 181 (1973) 547.
[19] B.H. Davis and P. Venuto, J. Catal. 15 (1969) 363.
[20] P. Mériaudeau and C. Naccache, Catal. Rev. Sci. Eng. 39 (1997) 5.
[21] J.M. Parera and N.S. Fígoli, in: *Catalytic Naphtha Reforming*, eds. G.J. Antos, A.M. Aitani and J.M. Parera (Dekker, New York, 1995) ch. 3.
[22] H.B. Davis, G.A. Westfall and R.W. Naylor, J. Catal. 42 (1976) 238.
[23] M. Boudart, A. Aldag, J.E. Benson, N.A. Dougharty and C.G. Harkins, J. Catal. 6 (1966) 92.
[24] G.A. Mills, H. Heinemann, T.H. Milliken and A.G. Oblad, Int. Eng. Chem. 45 (1953) 134.
[25] C.A. Querini, N.S. Fígoli and J.M. Parera, Appl. Catal. 52 (1989) 249.
[26] J.H. Sinfelt, J. Catal. 29 (1973) 308.